Hindawi

Research Article

Technoeconomic Analysis and Optimization of Hybrid Solar-Wind-Hydrodiesel Renewable Energy Systems Using Two Dispatch Strategies

Tiansheng Chen,[1] **Minglei Wang** [1] **Reza Babaei** [2] **Mohammad Esmaeili Safa** [3]
and Ali Asghar Shojaei [4]

[1]*Lanzhou College of Information Science and Technology, Lanzhou, Gansu Province 730000, China*
[2]*Department of Mechanical, Automotive & Materials Engineering, University of Windsor, Canada*
[3]*Department of Mechanical Engineering, Babol Noshirvani University of Technology, Babol, Iran*
[4]*Department of Electrical Engineering, Neyshabur Branch, Islamic Azad University, Neyshabur, Iran*

Correspondence should be addressed to Minglei Wang; lgz197409@163.com, Reza Babaei; babaeij@uwindsor.ca,
and Mohammad Esmaeili Safa; m.esmaeilisafa@stu.nit.ac.ir

Sustainable generation is impacted by the adoption of renewable energy, the growth of energy markets, and economic strategies. This paper offers a sustainable strategy and a technoeconomic analysis of off-grid hybrid energy systems (HES) in remote islands of Iran, including Lavan, Larak, and Failaka, utilizing PV module, wind turbine, and hydrokinetic turbines. Hourly wind speed, solar irradiation, and hydrovelocity have been implemented under load following (LF) and cycle charging (CC) dispatch strategies in order to ascertain the most appropriate systems. Lavan Island achieves the winning HES with a CC dispatch strategy, which consists of 3 hydroelectric turbines, 1 wind turbine, 349 kW of solar power, 150 kW of generator power, 316 kWh of batteries, and 287 kW of the converter. This ideal HES, which generates a consistent generation profile and reasonable net present cost (NPC) and cost of energy (COE) of M0.160$ and $0.013 kWh, respectively, can be practically attained in these areas. LF-controlled optimal solutions use less fuel than CC-based ones, leading to a higher share of renewable energy. Compared to Larak and Lavan, the CC- and LF-controlled options on Failaka Island generate cleaner electricity with emissions that are 57% and 44% lower. Regarding the ability to recoup the project's initial investment costs, long-term energy production would be more financially viable than short-term. Short-term projects with higher financial uncertainty due to the salvage cost should use the CC method.

1. Introduction

Over the past few decades, population growth, technological advancements, and new constructions have caused a sharp rise in electricity consumption. The total energy required is expected to increase by about 30% by 2040, compared to 2015. However, a large portion of the world population (~1.1 billion people) still lacks access to electricity, mostly in developing nations in Africa and the Middle East [1]. This dire situation prompted organizations and decision-makers to search for strategies that offer everyone long-term and sustainable electricity in these areas [2] to gradually turn to renewable energy and distributed energy systems to generate power [3].

Renewable energy sources can play a pivotal role in supplying electricity to remote localities. It is the desirable replacement for traditional energy because it is never-ending, and it has established its significance and won numerous significant privileges as a substitute for fossil fuels, which will eventually run out [4].

Nevertheless, power production reliability and consistency are recognized as the primary downsides of utilizing

renewable energy sources. This is due to fluctuations in solar irradiation, unanticipated variation of water velocity and inconsistency of wind intensity, the discrepancy in energy potential, and demand timings [5]. In this respect, hybrid energy systems (HES) were introduced as promising energy sources that combine renewable resources together to enhance system reliability, system efficiency, and profitability [6]. Renewable energy components in HESs operate together to benefit from multiple renewable resources, leading to more sustainable and compatible situations.

Conventional or fossil fuel-based energy sources account for about 75% of the power generated worldwide and substantially impact the energy market. The Middle East is one of the richest areas for oil and gas resources and utilization of sustainable applications might considerably influence the local and global economies [7–9]. Middle Eastern nations have planned to grow their sustainable policies and regulations in the future. Some potential areas in Iran particularly can are considered in this category for planning toward a sustainable future. Renewable applications integrated into the generator can be also appealing options in Iran due to a variety of government-funded fuel incentives, proper solar irradiation, and rising power demand [10]. One of the appealing areas in Iran is Persian Gulf and thus, the case areas of the article were selected from different geographical directions of Persian Gulf.

Persian Gulf in southern Iran is across the world's "Sun-Belt," which is the region that receives the highest solar irradiation. Some remote places in the Persian Gulf, such as the islands of Lavan, Larak, and Failaka, rely on a long underwater cable with an unstable energy supply and frequent blackouts when people most require it, mainly during the summer months. In these places, single-phase electricity transports less energy than three-phase power, resulting in lower service and life quality for people. Each year, these remote islands in the Persian Gulf reach about 300 sunny days, higher than 20 GW wind power potential, and a decent water velocity [11].

The Iranian government acknowledged the importance of sustainable power foundations and is slowly initiating the facilities and pricing policies required to encourage private sector investment. According to Iran's 5th development plan, renewable energy generation reached 5000 MW in 2015. Nonetheless, the perspective was not satisfied because of severe economic sanctions and a lack of foundation and equipment in the sustainable power sector [3]. The parliament then approved the sixth development perspective, aiming to meet this goal by 2021 and generate more than 2500 MW of electricity by 2030. By 2025, clean power foundations are estimated to meet 10% of Iran's total energy needs [12].

Several viable clean infrastructures are employed to activate the availability of sustainable energy in Persian Gulf. Photovoltaic (PV) arrays are the most common renewable components due to their cheap maintenance and operation, expenses, and ease of use to meet rising energy demands [13]. The solar electricity generated varies based on the amount of irradiation received at the location. Because wind turbines (WT) are proportional to wind intensity, they are

also a viable solution for coastal areas. On the other hand, wind power generation might fluctuate significantly from month to month [13]. Furthermore, hydrokinetic (HKT), which utilizes water velocity to supply power, is a promising clean energy technology for onshore communities with adequate water resources. However, the volatile nature of renewables and the significant fluctuation in load demand necessitate the use of a generator, which offers financial benefits in the Middle East due to diesel's lower price [14–16]. Until recently, very limited attention has been drawn to support the use of renewable HES to deliver electricity in the Persian Gulf's isolated islands. However, some studies pertinent to showing the technoeconomic feasibility analysis of HES in various parts of this country are summarized in Table 1.

Controlling energy management through battery and DG is necessary to maximize the power reliability of HES. A controlling algorithm or dispatch strategies can be implemented to manage the system, boost system effectiveness, and reduce investment [23]. A proper dispatch strategy prevents overload damage to components, maximizes cost efficiency, ensures energy continuity, and improves power efficiency. The control algorithm must be appropriate for the load characteristics in the target area in order to obtain the best HES design [12].

One of the most popular and precise approaches for using a dispatch strategy is to use artificial intelligence. HOMER PRO is a prominent software used for its high speed and accuracy in identifying the best options. HOMER PRO determines feasible sizes of winning HES according to the input parameters such as load data, resource availability, and economic and technical specifications of energy systems. There are multiple dispatch strategies in HOMER, including combined dispatch (CD), cycle charging (CC), generator order (GO), predictive dispatch (PD), load following (LF), and the user's own control strategy, all of which are designed using the MATLAB ink function. For instance, Reference [24] studied the impacts of various strategies for a HES involving PV/WT/DG/hydro in a rural locality of India. The results represented that the CD controller obtained the cheapest COE ($0.31/kWh), and the LF strategy achieved the highest renewable penetration in comparison with the other techniques. Similar to this, Refeerene [25] investigated technoeconomic viability analysis of PV/WT/battery/biogas generator systems utilizing different dispatch strategies. The results showed that the CD method could economically meet the load demand if the HES comprised 0.5% biofuel, 12.7% wind energy, and 86.8% solar energy. Reference [23] revealed that the CC-based energy systems consume more fuel than LF-based options, and the combination of CC-controlled systems achieved M0.160$, $0.013 kWh, and 26% higher NPC COE, and the renewable fraction, respectively, than that of LF-controlled system. The LF-based strategy in Reference [26] obtained the highest PV output of 51.1% with the fuel of wood residue in the gasifier, while the CC-based option is more equitable with a slightly higher percentage of HKT by 52% using a wood, cane, and cocoa-fired gasifier. Also, the study mentioned that the CC method minimized the financial indicators of the optimal solution more than other strategies.

TABLE 1: Summary of the technoeconomic feasibility analysis of HES in Iran.

Ref., year	Area (≅peak load)	Optimization method	Optimal solution	Outputs
[17], 2020	Anzali, Genaveh, Jask (8,258.16 kW)	HOMER strategy	For Anzali: PV: 7,221 kW WT: 14 units with 660 kW Battery: 454 units(167 ah)	NPC: $48.8 M COE: $0.242/kWh RF: 100%
[18], 2019	Damghan (1 kW)	HOMER strategy	PV: 1,430 kWh/yr WT: 8,353 kWh/yr DG: 3,009 kWh/yr	COE: $0.338/kWh RF: 76.5%
[19], 2019	Bandar Abbas, Shiraz, Tabriz, Tehran, Yazd (370.34 kW)	HOMER strategy	In Tehran: PV: 997 kW WT: 7 units with 95 kW DG: 1,000 kW ELC: 120 kW HT: 130 kg Battery: 9 units(130 kWh)	In Tehran: COE: $0.340/ kWh RF: 24.7%
[20], 2019	Rayen (79.56 kW)	HOMER strategy	PV: 28.7 kW WT: 14 units with 1.5 kW DG: 30 kW Battery: 18 units (7.55 kWh)	NPC: $268.6 k COE: $0.197/kWh RF: 67.3%
[21], 2018	Kerman (3.3 kW)	HCHSA strategy	PV: 7 units with 0.120 kW WT: 6 units with 1 kW Battery: 7 units(1.35 kWh)	Life cycle cost: $4 k
[22], 2018	Fedeshk, South Khorasan (7.5 kW)	Hybrid strategy	PV: 77 m^2 (~48 units with 0.26 kW) Battery: 29 units(2.1 kWh) Biodiesel: 9.8 kW	Life cycle cost: $20 k

Some other relevant studies of the technoeconomic feasibility of HES have focused on three major groups, comparison procedures [27], design and planning [28–30], and energy management [31, 32]. The project lifetime in all of these research articles has been set at 20 or 25 years, with no consideration of the impacts of reducing the project's lifetime. The remaining value of the components rises as lifetime shortens, which can be an effective consideration in financing renewables in a place. The sizing analysis of storage devices in a hybrid electric car was explored in Reference [33]. The results showed that the salvage cost of the batteries had a substantial impact on the system's annual cash flow. Reference [34] designed a large-scale off-grid HES for a rural area in Nigeria. The optimum option obtained a 1.5 MW PV, 350 kW DG, and 1,200 batteries with an NPC of $4,909,206 and a COE of $0.396/kWh. The findings of the paper demonstrated that the ratio of the salvage value to the capital cost of the PV, DG, battery, and converter was roughly 15.6%, 13.1%, 20.1%, and 6.5%, respectively. According to the findings, the salvage value of the initial investment of the PV, DG, battery, and converter was observed to be roughly 15.6%, 13.1%, 20.1%, and 6.5%, respectively. For total initial expenses of $3,013,486, roughly $485,724 of salvage costs appeared when the project was completed. Reference [35] investigated the best configuration of a standalone hybrid photovoltaic/battery energy storage system using the effective metaheuristic algorithm, improved harmony search to supply electricity to a residential load in Iran. Reference [36] designed a PV/DG system for a small-scale load profile. They also mentioned if initial expenses of $26,150 are invested, the salvage cost will equal $2,300. Reference [37] noted that the PV/biomass system uses the most recent GPC optimization method to get the lowest cost of investment. A comparison between the devised algorithm and the AEFA and GWO algorithms is made. The goal is to reduce the net present cost while still adhering to specific technological limitations. Reference [38] also pointed out a novel optimization technique for the best Bio/PV/WT microgrid design, considering various economic and environmental factors. The backtracking search algorithm (BSA) and the invasive weed optimization (IWO) are two metaheuristic algorithms that were combined to create the newly developed optimization algorithm. The results indicated that, when using the suggested IWO/BSA algorithm, PV/biomass and PV/diesel/battery systems have the lowest energy costs, with respective costs of $0.1184/kWh and $0.1354/kWh. Despite the significance of salvage in the technoeconomic feasibility analysis of HES, none of these previous papers has undertaken a sensitivity analysis on this value.

Based on what has been reviewed in Table 1 and other literature, the possible gaps include:

(i) In Iran, hydrokinetic turbines have not received as much attention as other more widely used

renewable energy sources despite being one of the cleanest and most recently developed generating units

(ii) The project lifetime of all papers presented has been set at ≥20 years; however, the impact of reducing the project duration on ROI, energy cost, and a renewable fraction has not been studied yet

(iii) There is also a lack of studies that paid attention to the impact of battery SOC_{min} variation on the financial, technical, and environmental aspects of clean energy solutions

Thus, the objective of the analysis is to discover a combination of clean energy foundations that can address the long-term power needs of rural areas in the Persian Gulf. Hourly water velocity data, wind speed, irradiation intensity, and fuel cost variations are all effective factors in the simulation. Two energy management control strategies, containing LF and CC, are used to smooth energy delivery, boost reliability, and lower the cost. Using HOMER, the best strategy is presented according to their technoeconomic-environmental aspects. The contributions of the present study are to (i) offer technically, financially, and environmentally winning CC- and LF-controlled HES with DG, PV, WT, HKT, and battery in isolated islands of Persian Gulf, (ii) compare impacts of the project lifetime, SOC_{min}, and dispatch strategies on the profitability and sustainability of the renewable solutions, and (iii) predict impacts of the controlling strategy and project lifetime on salvage value and ROI fluctuation. This would be the first research to represent standalone renewable solutions as viable alternatives in the Persian Gulf island.

This article contains six main sections commencing with (i) identifying feasible and economical renewable HES, (ii) representing the financial (cost breakdown and ROI), technical (generator and battery status), and environmental (gas emissions) of each optimal solution under two dispatch strategies, (iii) contrasting the technical, economic, and environmental results in two dispatch strategies, (iv) carrying out a sensitivity analysis to find out how SOC_{min}, project lifetime, and renewable resources affect system parameters, and (vii) demonstrating the difference of energy delivery and flows under control of CC and LF controllers.

2. Methods and Materials

2.1. Introduction of the Intended Areas. Two rural areas on isolated islands are considered in this analysis: Larak Island, Failaka Island, and Lavan Island, situated in separate positions in Persian Gulf, as shown in Figure 1. Table 2 presents the condition of the intended islands. Iran controls the territory of Larak and Lavan Island, and Kuwait governs Failaka. The area of Failaka and Lavan is roughly double the Larak's area. The climatic condition follows a fairly similar annual pattern of hot and dry conditions in these places. Fialka and Larak have longer and shorter distances from the nearest grid infrastructures, respectively. Figure 2 displays monthly meteorological data of the selected islands. Wave

energy data per month and climatic characteristics of Persian Gulf were derived from Reference [39] and NASA [40], respectively. In all seasons except summer, the average environmental temperature on Larak Island is greater than in the other areas. In June, Failaka Island receives an average of $8 \, kWh/m^2/d$ of solar irradiation, which drops to under $4 \, kWh/m^2/d$ in the winter. Summer is the windiest season, resulting in a higher wave velocity of up to $4 \, m/s$.

2.2. Description of Load Profile. Table 3 depicts an approximate scenario for various appliance usages daily, which can be used by roughly 200 residential households in the case areas. These residential buildings are designed for a normal family of five with a low-income stream. The load demand was measured by personal meter reading in other electrified places with similar remote conditions and household statuses. The hourly load demand of an average household is represented in Figure 3 based on the considered loads. Here, deeming the hot-dry climate classification of the case areas, it is apparent that the energy demand peaked over the summer, which can be due to increased working hours, higher utilization of cooling systems, more tourists coming to these areas. The annual peak hours mostly start from 8 a.m. to 8 p.m. ranging from 170 kW to 2120 kW. The minimum energy consumption also is observed to be under 70 kW, from 8 p.m. to 5 a.m.

2.3. Dispatch Strategy. This research allows users to find suitable clean power combinations and build a decent integration to meet load needs. Therefore, hybrid power solutions are simulated using the adopted dispatch strategies, such as CC and LF controllers. The optimizer starts by doing a precise optimization assessment for each hybridization case, calculating cost savings, reliability gains, and pollution reductions CC or LF strategies are implemented when the components such as battery and generator operate together to satisfy load demand during a time step [42].

2.3.1. LF Dispatch Strategy Description. In the LF method, DG works to produce sufficient power to meet the required load. The lower-priority goals, such as batteries, will continue to be charged by renewable energy sources [43]. The dispatch strategy only permits the battery to be charged by excess energy generated by renewable energy sources (PV, HKT, and WT). It stops the battery from being charged by the DG. As a result, the diesel generator is provided with enough power to satisfy the unmet load. The LF method's algorithm is shown in Figure 4. During high-load periods, the LF method considers that using DG is necessary. The LF control technique, on the other hand, is deemed inefficient if the DG continues to operate at low loads in the following periods.

(i) When the total renewable energy produced equals the required load ($P_{RE} = P_L$), the first condition occurs. The renewable sources (PV/HKT/WT) supply the required load in this case. The DG is shut off, and the battery units are not charged. In this case, there is no excess electricity

FIGURE 1: The location of the intended islands on the map of Iran and Persian Gulf.

TABLE 2: General description of the intended islands.

Island	Direction in Persian Gulf	Coordinate	Area (km^2)	Whether type	Distance to the nearest grid (km)
Larak	Eastern	26.84° N 56.37° E	85	Extremely hot-dry	12
Lavan	Middle	26.80° N, 53.27° E	50	Hot-dry	18
Failaka	Western	29.44° N 48.28° E	45	Very hot-dry	20

(ii) When the total renewable energy produced exceeds the required load ($P_{RE} > P_L$), the second condition occurs. The renewable components meet the load requirement, resulting in a power surplus. When the battery is charged, the surplus energy is discharged. Excess renewable energy is used to charge the battery if it is not fully charged

(iii) When total renewable energy is lower than the required load ($P_{RE} < P_L$), the last situation occurs. The possible two subcategories are as follows

   (a) The DG meets the net load demand if SOC = SOC$_{min}$ (load minus renewable output). The DG only generates sufficient power to meet the net load; therefore, the battery remains unchanged. The DG will meet the load demand if the minimum DG output power exceeds the net load, while the PV/HKT/WT will charge the battery

   (b) The price of depleting the battery is measured and assessed by operating the DG, which merely meets the net load requirement if SOC > SOC$_{min}$. If the expense of draining the battery is greater than starting a DG, the battery will not be drained while the DG is running, and DG will generate enough energy to supply the required load without having to charge the battery

The mathematical descriptions of the LF dispatch strategy are discussed below.

(i) If the total power generated from PV, HKT, and WT is sufficient, and SOC(t) < SOC$_{min}$(t) simultaneously, the load is supplied by renewable components

$$P_{load}(t) = P_{WT}(t) + P_{HKT}(t) + \frac{P_{PV}(t)}{\eta_{inverter}}. \quad (1)$$

Then, the excess energy produced from the renewable suppliers serves to recharge the battery pack.

$$P_{battery}(t) = P_{WT}(t) + P_{HKT}(t) + \frac{P_{PV}}{\eta_{inverter}} - P_{load}(t). \quad (2)$$

(ii) If the total power generated by PV, HKT, and WT is enough and SOC(t) ≥ SOC$_{min}$(t), excess electricity must be deferred

(iii) If the overall energy provided by PV, HKT, and WT is inadequate, SOC(t) < SOC$_{min}$(t), the energy to satisfy the primary is supplied by DG at the energy needed to meet the load demand
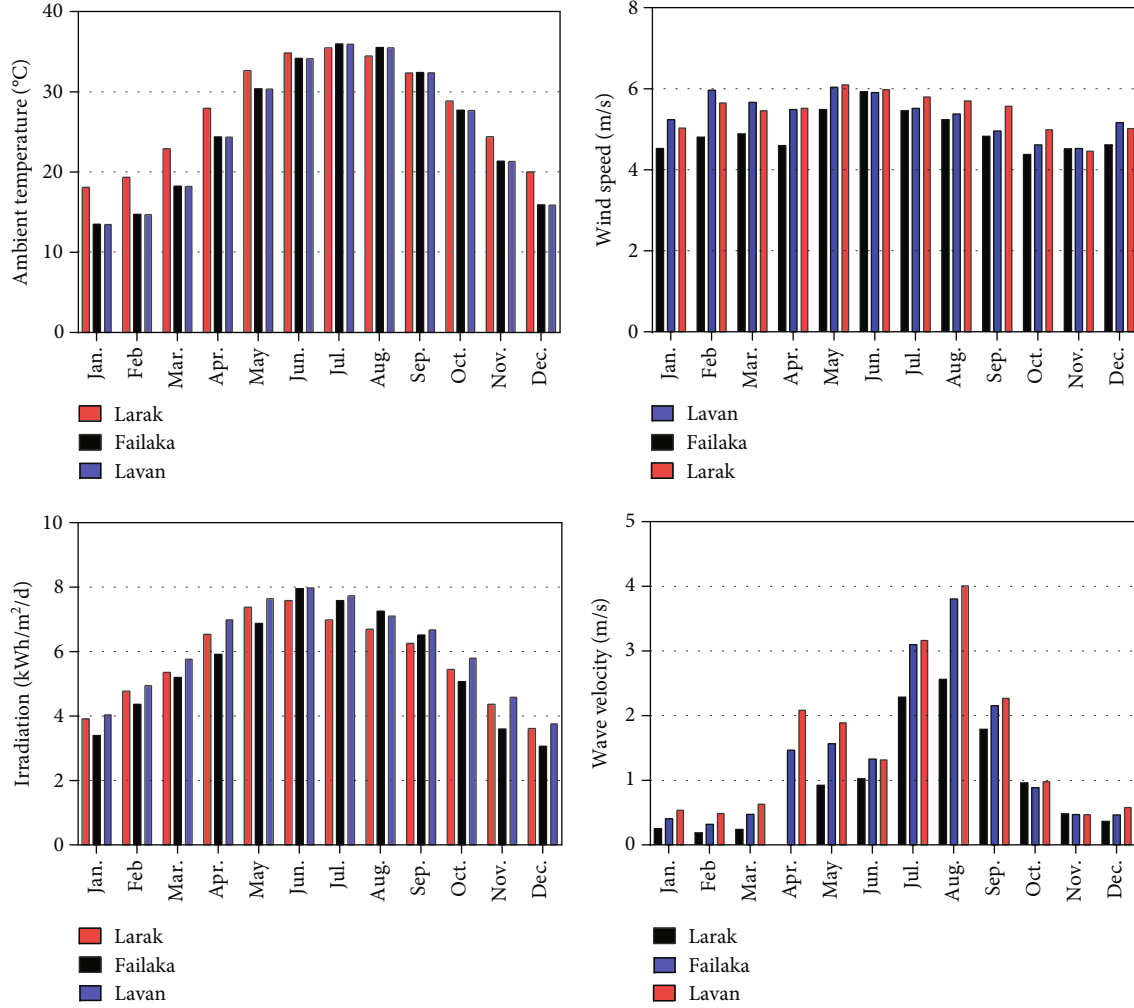
Figure 2: Monthly weather data of the selected islands.

Table 3: Estimation of the primary load of the intended area [41].

Appliance	Rating per quantity (W)	Quantity	Daily operating time (h/day)	Daily demand (kWh/d)
Fridge	20	200	24	96
Freezer	90	180	24	388.8
TV	80	220	5	88
Ceiling fans	30	250	3	22.5
Air conditioner	735	250	8	1470
Washing machine	500	180	1	90
Light bulbs	40/60	1200	5	300
Miscellaneous*	N/A	N/A	24	0.28
Total	—	—	—	2,455

*Embodies small objects such as small equipment, charging devices, and temporary use of other appliances (e.g., radios, TV, and kettle).

$$P_{\mathrm{DG}}(t) = P_{\mathrm{load}}(t). \tag{3}$$

(iv) When the energy produced by PV, HKT, and WT is inadequate and $\mathrm{SOC}(t) \geq \mathrm{SOC}_{\min}(t)$, the required

power to satisfy the load demand is supplied by renewable sources and battery pack

$$P_{\mathrm{load}}(t) = P_{\mathrm{battery}}(t) + P_{\mathrm{HKT}}(t) + \frac{P_{\mathrm{PV}}(t)}{\eta_{\mathrm{inverter}}}. \tag{4}$$
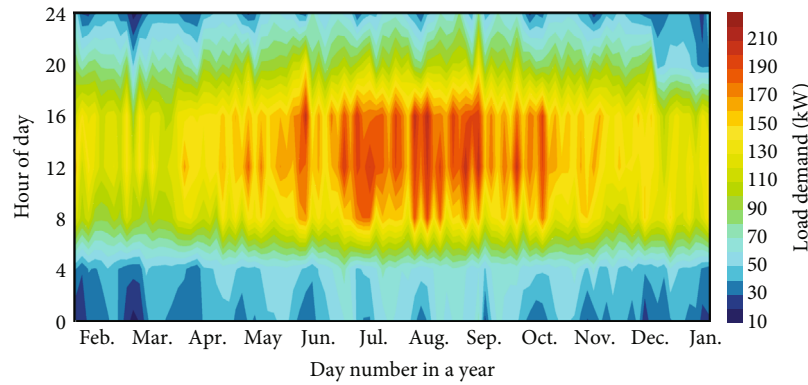
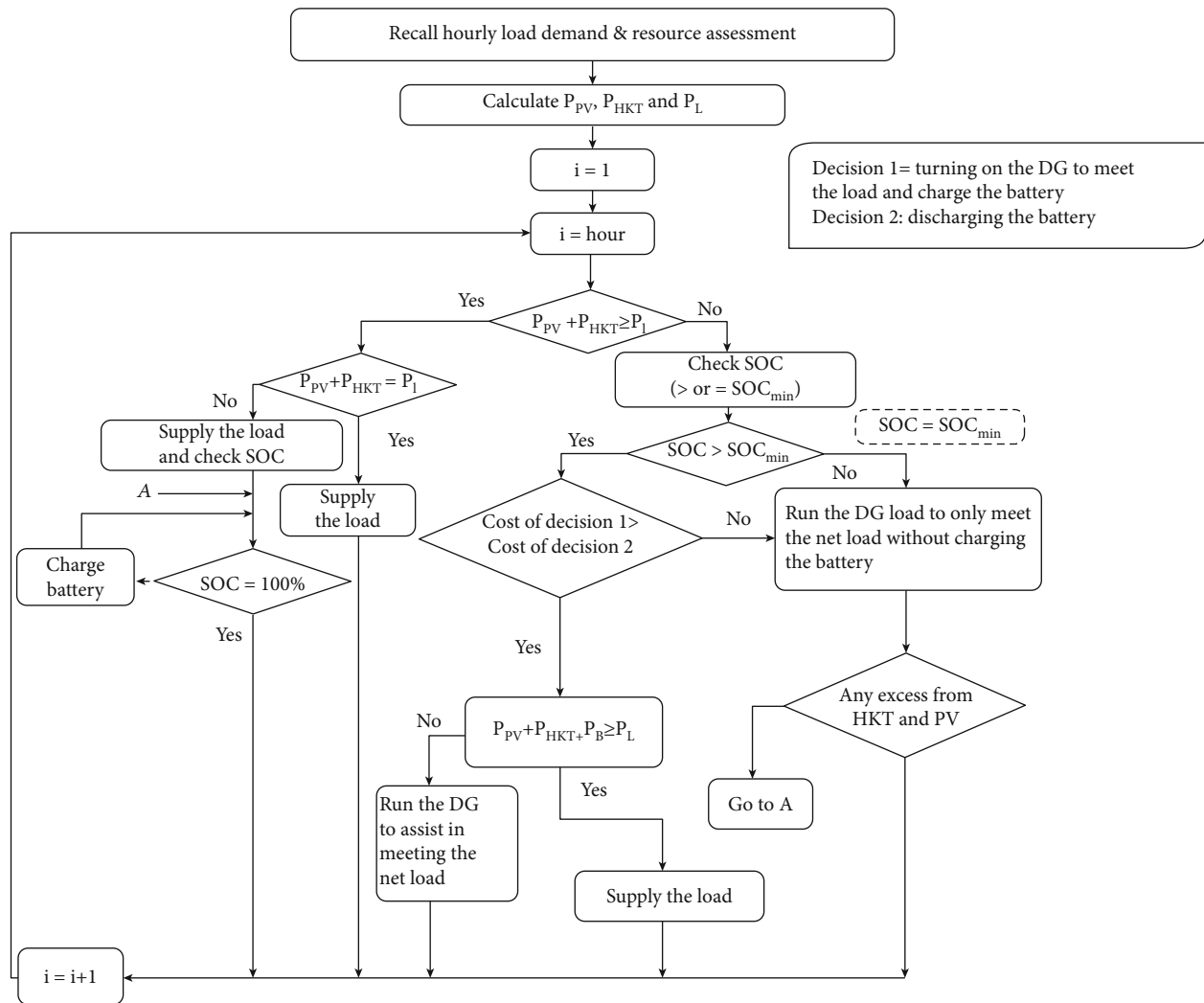FIGURE 3: The annual hourly load profile of the considered islands.

FIGURE 4: LF algorithm description for the PV/WT/DG/battery HES.

2.3.2. CC Dispatch Strategy. The DG utilizes its full rated capacity to fulfill the required load in the CC dispatch strategy, and any excess electrical generation is used for lower-priority tasks such as charging battery packs. Therefore, once the DG starts charging the battery, it constantly goes until the SOC set point is met. Figure 5 depicts the cycle charging (CC) control strategy's algorithm. This system uses the same operational technique as the LF dispatch system. CC strategy is different from the LF strategy; whenever the DG is turned on, it runs at its full capacity to meet the net load while also charging the battery.
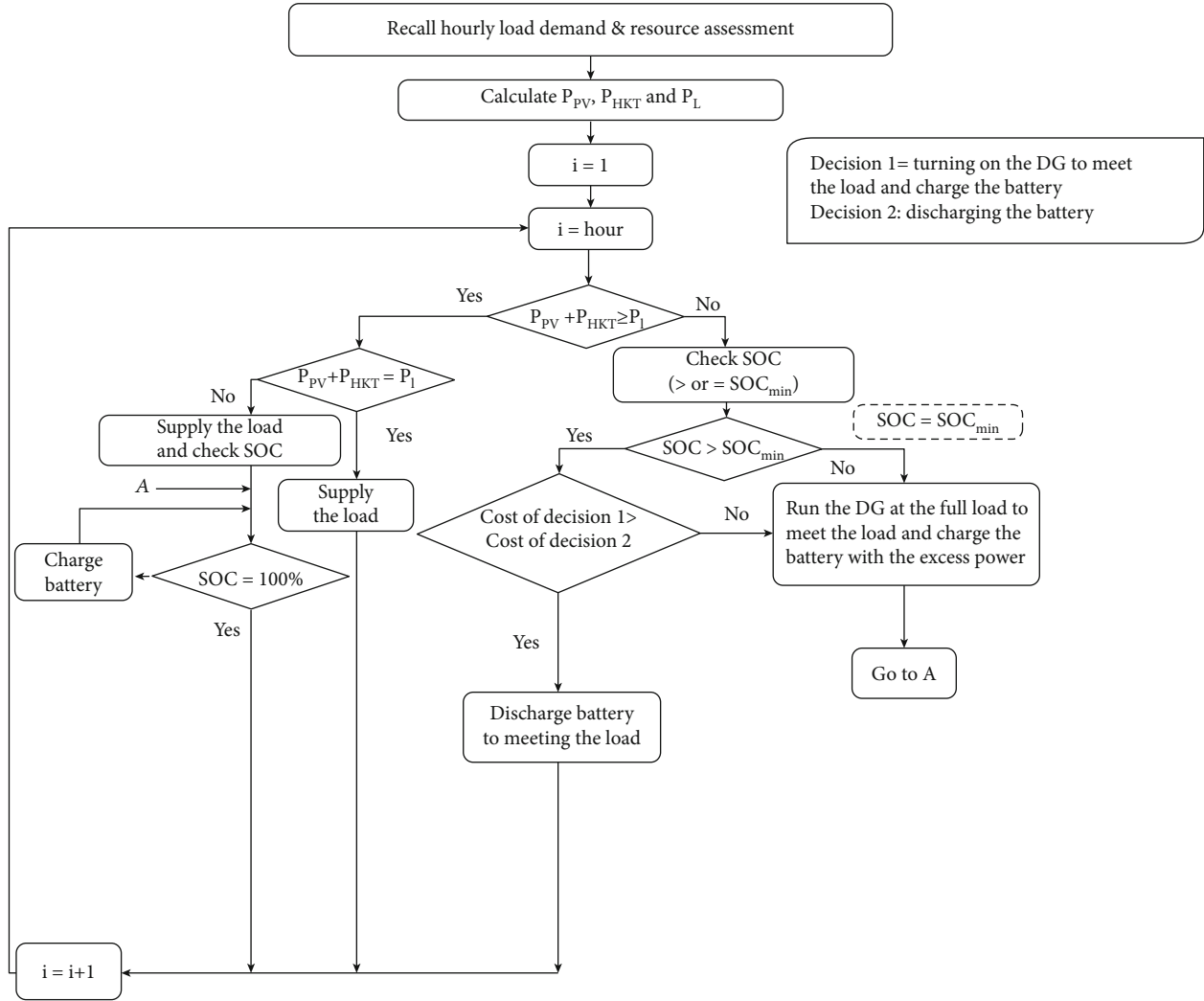
FIGURE 5: CC algorithm description for the PV/WT/DG/battery HES.

The operation of the CC controller is discussed below.

(i) If the overall power generated from PV, HKT, and WT is sufficient, and $SOC(t) < SOC_{min}(t)$ simultaneously, the load is supplied by renewable components, and the battery is charged with the DG at full capacity

$$P_{load}(t) = P_{WT}(t) + P_{HKT}(t) + \frac{P_{PV}(t)}{\eta_{inverter}}, \qquad (5)$$

$$P_{battery}(t) = P_{max,DG}(t). \qquad (6)$$

(ii) If the total energy generated by PV, HKT, and WT is adequate and $SOC(t) \geq SOC_{min}(t)$, excess electricity is deferred

(iii) If the overall energy provided by PV, HKT, and WT is inadequate and $SOC(t) < SOC_{min}(t)$, the energy to satisfy the load demand is supplied by DG at its full power to meet the load demand

$$P_{battery}(t) = P_{max,DG}(t) - P_{load}(t). \qquad (7)$$

(iv) When the energy generated by PV, HKT, and WT is insufficient and $SOC(t) \geq SOC_{min}(t)$, the required power to meet the load demand is supplied by renewable sources and batteries

$$P_{load}(t) = P_{battery}(t) + P_{HKT}(t) + \frac{P_{PV}(t)}{\eta_{inverter}}. \qquad (8)$$

2.4. Description of the Hybrid Energy Solution. The intended design in this study is influenced by either renewable or fossil fuel-based power generation sources. The balance of power over a year (8760 hours) is of the utmost priority. Thus, each piece of equipment is mathematically represented, and the amount of power produced and stored by each component is computed. Figure 6 presents the configuration of the HES assumed to electrify 200 residential households in the considered areas. To provide uniform and stable electricity, PV solar panels, wind turbine (WT), and hydroturbine (HKT) are connected with generators (DG), battery packs, and inverters. Tables 4 and 5 also provide the important technical and financial parameters relevant to this equipment.

2.4.1. Generator. The use of diesel generators (DG) in grid-isolated options assists in supporting load peaks first, then reduces the need for battery units, resulting in cost savings. The following equation expresses the DG's efficiency according to the lower heating value (LHV) [48]:

$$\eta_{DG} = \frac{3.6 P_{DG}}{GHC.LHV_D}. \tag{9}$$

Here, GFC is the generator fuel consumption rate, P_{DG} is the output power (kW), LHV_D is the calorific value of diesel based on water vapor, and P_{DG} is the rated generator power (kW). The following equation shows the hourly generator's fuel consumption (L/h) as a function of its electrical output [72]:

$$\dot{m}_{fuel} = F_0 Y_{DG} + F_1 P_{DG}. \tag{10}$$

Here, Y_{DG} is the DG output (kW), F_0 is the fuel curve intercept coefficient (L/h/rated kW or m³/h/rated kW), and F_1 is the fuel curve slope (L/h/output kW or m³/h/output kW). The fuel curve intercept coefficient can be defined as the noload fuel consumption of the generator divided by its rated capacity. The fuel curve is the slope marginal fuel consumption of the generator, in units of fuel per hour per kW of output, or equivalently, units of fuel per kWh.

2.4.2. Wind Turbine. At rated wind speed, the wind's kinetic energy is converted into mechanical energy by rotating the turbine blade, which is subsequently converted into electricity via the shaft attached to the alternator [43]. In determining the output of a wind turbine, the power curve is critical. The following equations are used to calculate energy output in most wind turbine applications [17].

$$P_{WT=} \begin{cases} P_{rated} \left(\dfrac{v^3 - v_{Cutin}^3}{v_{Rated}^3 - v_{Cutin}^3} \right) & v_{Custin} < v \le v_{Rated}, \\ P_{Rated} & v_{Rated} < v \le v_{Cuttoff}, \\ 0 & v > v_{Cuttoff} \text{ or } v < v_{Cuttoff}, \end{cases} \tag{11}$$

where P_{rated} is the rated power of the wind turbine (kW), V is the wind speed (m/s), v_{Rated} is the rated wind speed, v_{Custin}

is the cut-in wind speed, and $v_{Cuttoff}$ is the cut-off wind speed, and the effective electrical power output is determined by the equation as follows [49]:

$$P_{e,WT} = P_{WT}.A_{WT}.\eta_{WT}. \tag{12}$$

Here, A_{WT} is the swept area of the turbine and $.\eta_{WT}$ is the wind turbine efficiency.

2.4.3. PV Module. Environmental factors (ambient temperature, clearness index, humidity, etc.), solar irradiation (kWh/m²/day), and collector technology all affect the performance of a PV array. The derating factor is a scaling factor that takes into account the effects of dust temperature, snow cover, wire losses, and aging [50]. The following equation can be used to calculate the PV module's output energy [20]:

$$p_{PV} = W_{PV} f_{PV} \frac{G_T}{G_S} \left[1 + \alpha_p (T_C - T_S) \right]. \tag{13}$$

Here, W_{pv} is the peak output of the PV array (kW), f_{pv} is the PV derating factor (%), G_T is the irradiation incident in the current hour (kW/m²), G_S is the incident irradiation at standard test conditions (1 kW/m²), and α_p is the temperature coefficient (%/°C). T_C is the panel temperature (°C) and T_S is the PV module temperature in the test condition (°C).

2.4.4. Hydrokinetic Turbines. The velocity of the water determines the properties of hydrokinetic turbines. The longitudinal system (which is vertically oriented in the direction of the waves in water) takes the energy from the waves and converts it into electricity. The generated energy is then converted to shore using proprietary equipment and cables [51]. Equation (6) presents the full obtainable energy from sea waves [52].

$$P_{max} = \frac{\rho g^2 TH^2}{64\pi} \times L_{max}. \tag{14}$$

Here, P_{max} is the maximum available power, ρ is the water density, g is the gravitational acceleration, T is the wave period, H represents the significant wave height, and L_{max} is the absorption width in maximum power.

2.4.5. Battery and Converter. Li-ion batteries are commonly used as a system backup because of their stability, long-term efficiency, high depth of discharge (DOD), and flexibility. It facilitates the system in storing the energy generated by components to be used at unpredictable times. The maximum stored energy can be measured by [53]

$$P_{Batt,C\ max} = \frac{\min (P_{Batt,C\ max,kbm} P_{Batt,C\ max,mcr} P_{Batt,Cmax,mcc}}{\eta_{Batt,C}}, \tag{15}$$

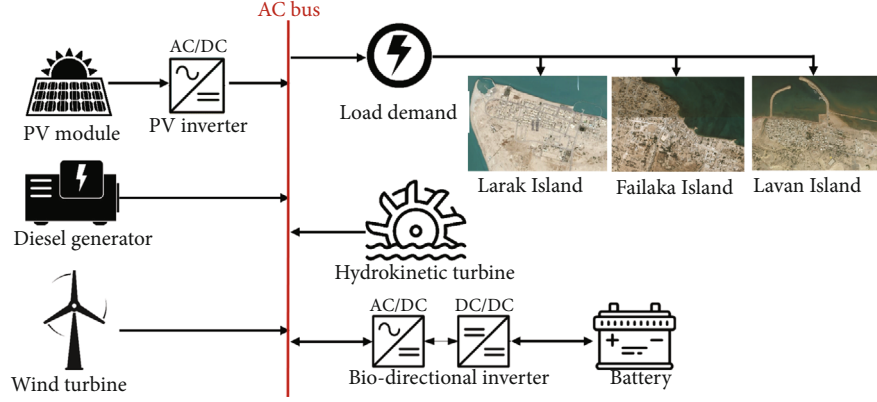where $\eta_{Batt,C}$ is the efficiency of charge storage,

FIGURE 6: Schematic layout of the considered HES in intended islands.

TABLE 4: Technical characteristics of the component in the intended hybrid energy system.

Component	Parameter	Value
PV system	Rated capacity (kW)	1
	Temperature coefficient	-0.4
	Operating temperature (°C)	25
	Derating factor (%)	80
	Panel area (m^2)	1.627
	Efficiency (%)	19.1
Wind turbine	Rated capacity (kW)	10
	Hub height (m)	24
Hydrokinetic turbine	Rated capacity (kW)	20
	Rotor diameter (m)	1.54
	Required water depth (m)	3
	Weight (kg)	750
	Size (m^2)	7
Diesel generator	Rated capacity (kW)	150
	Minimum load ratio (%)	25
	Minimum load ratio (%)	0.25
Converter	Relative capacity (%)	100
	Inverter/rectifier efficiency (%)	95
Battery storage	Nominal voltage (V)	6
	Nominal capacity (kWh)	1
	Minimum state of charge (%)	20
	Maximum charge current (A)	167

$$P_{\text{Batt},C\,\max,\text{kbm}} = \frac{kQ_1 e^{-k\Delta t} + Qkc\left(1 - e^{-k\Delta t}\right)}{1 - e^{-k\Delta t} + c\left(k\Delta t - 1 + e^{-k\Delta t}\right)}, \quad (16)$$

$$P_{\text{Batt},C\,\max,\text{mcr}} = \frac{\left(1 - e^{-\alpha_c \Delta t}\right)(Q_{\max} - Q)}{\Delta t}, \quad (17)$$

$$P_{\text{Batt},C\,\max,\text{mcc}} = \frac{N_{\text{Batt}} \cdot I_{\max} \cdot V_{\text{nom}}}{1000}, \quad (18)$$

where k is the constant of storage rate (h^{-1}), Q_1 is the available energy remaining at the first time step (kWh), Δt is time step duration(h), Q is the energy available in the storage at the first time step (kWh), c is the capacity ratio of storage, α_c is the maximum battery charge (A/Ah), $Q_{\max}$ is the total battery capacity (kWh), N_{Batt} is the number of batteries, $I_{\max}$ is the battery's maximum storage current (A), and V_{nom} is the battery's nominal voltage.

In order to harmonize hybrid energy systems, the system converter is crucial. The main function of a converter is to keep the energy flowing between AC and DC. It acts as a medium for converting DC to AC electric power and serves as a link between the two systems by converting DC to AC. The power rating of the converter is expressed by [20]

$$P_{\text{inv}}(t) = \frac{(\rho/\rho_0) \cdot P_{\max.L}(t)}{\eta_{\text{inv}}}, \quad (19)$$

where $P_{\max.L}$ is the required load demand and η_{inv} is the inverter efficiency.

2.5. Financial Parameters. The net present cost is the sum of all initial, operation, maintenance costs, replacement, and fuel costs, less the salvage cost at the end of the project's life cycle [54]. To calculate the total NPC of HES, the following equation is utilized [51]:

$$C_{\text{npc,tot}} = \frac{C_{\text{ann,tot}}}{\text{CRF}\left(i, R_{\text{proj}}\right)}, \quad (20)$$

where $C_{\text{ann,tot}}$ is the yearly cost ($/year), i is the interest rate (%), T_P is the project lifetime (year), and CRF is the capital recovery factor, which is determined by the equation as

$$\text{CRF}(i, n) = \frac{i(1 + i)^n}{(1 + i)^n - 1}. \quad (21)$$

TABLE 5: Financial input parameters of considered HES.

Equipment	Initial expense ($/kW)	Replacement expense ($/kW)	Lifetime (year)	Ref.
PV system	650	650	30	[44]
Wind turbine	1,450	1,450	20	[45]
Hydrokinetic turbine	1,300	870	15	[24]
Generator	350	350	15,000 hrs	[46]
Battery	200/kWh	180/kWh	15	[47]
Converter	300	300	15	[19]

TABLE 6: Results of optimization analysis of the HES in each island.

	Parameter	Unit	Larak Island		Failaka Island		Lavan Island	
			CC	LF	CC	LF	CC	LF
Component	DG	Size (kW)	150	150	150	150	150	150
		Fuel use (L/year)	90,661	18,223	39,544	6,745	81,037	19,159
	PV system	Capacity (kW)	443	668	568	1,056	349	594
	Battery	Size (kWh)	350	1,249	1,145	1,424	316	918
		Autonomy (hr)	2.80	9.88	9.06	11.3	2.5	7.26
	Converter	Size (kW)	280	274	306	323	287	300
	HKT	Quantity (no.)	2	2	2	2	2	2
		Activity (h/year)	2,928	2,928	4,392	4,392	4,392	4,392
	WT	Quantity (no.)	1	1	1	1	1	1
		Activity (h/year)	6,559	6,559	6,160	6,160	6,504	6,504
Generation	RF	(%)	63.9	93.6	84.2	97.7	67.8	93.6
	Excess electricity	MWh/yr	205.8	331.3	253.3	979	67.8	93.6
	Capacity shortage	kWh/yr	878	701	445	866	855	853
	Total energy generation	MWh/yr	1,148	1,285	1,208	1,932	1.089	1,280
	Unmet load	kWh/yr	136	31.2	7.8	242	7.52	13.9

Here, n is the project lifetime (year) and i is the yearly interest rate, which is measured by [52]

$$i = \frac{i^{\circ} - f}{1 + f}, \qquad (22)$$

where i° if is the annual inflation rate (%).

(i) Operating cost (OC): this cost determines by subtracting the total yearly cost from the capital investment, specified by the following equation [55]:

$$OC = C_{ann,tot} - C_{ann,capital}. \qquad (23)$$

(ii) Energy cost (COE): the critical metrics for comparing the hybrid system's economic parameters. The COE is calculated by dividing the average cost of a HES by the total served electricity (kWh), which would be calculated using the following [56]:

$$COE = \frac{C_{ann,tot}}{L_{ann,load}}. \qquad (24)$$

Here, $L_{ann,load}$ is the electricity use per year (kWh/year) and $C_{ann,tot}$ is the total annual cost ($/year).

3. Results and Discussion

This section summarizes the financial, technical, and environmental findings of the optimum sizes. The outputs of the sensitivity analysis will be followed by a more detailed explanation of the optimum simulated systems in each island. Afterward, the comparison of the present work's optimal case, its winning dispatch strategy, and outputs is carried out with the relevant literature.

3.1. Optimal Decision-Making in Each Area. Several technically and economically feasible renewable solutions on each island in LF and CC methods were identified, each including unique features. A feasible HES can generate sufficient electricity and satisfy annual load requirements at the same time. The infeasible cases which are not able to satisfy the user-specified parameters will be removed for the pom the
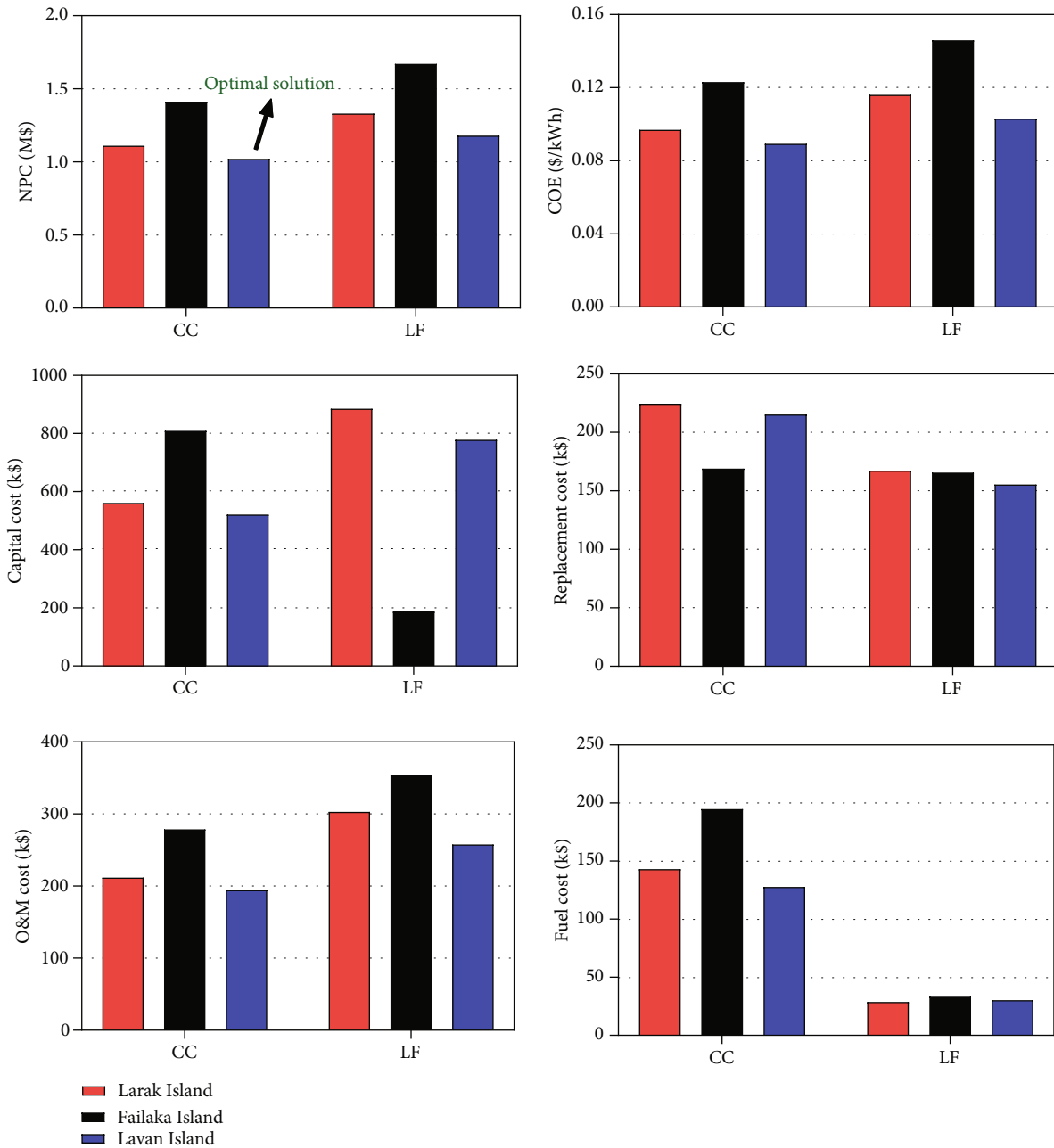
FIGURE 7: Financial parameters of the optimal solutions in the CC and LF strategies.

potential options. The remaining feasible systems are categorized based on the NPC. Table 6 presents the optimal system sizes of the considered islands in CC and LF strategies. Despite utilizing two hydroturbines in all feasible options, Larak Island has the lowest operation hour, meaning that other components, especially PV panels, are more active in Larak.

The LF-based system in Failaka has higher autonomy hours, more PV arrays, and lower diesel use. The CC-controlled options use higher fuel than LF-controlled solutions and are anticipated to have a lower fraction of renewable output. In more detail, the difference between the renewable fraction of CC- and LF-based solutions ranges from 12.8% to 29%. Furthermore, the PV panel in LF-

controlled HES of Failaka is the best option for generating yearly electricity, which is 1931.9 MWh/year. Because of the relatively similar wind intensity on the islands and the higher initial expenses of wind turbines in the Middle East, all the optimum options use only one wind turbine.

3.1.1. Cost Breakdown and ROI. Figure 7 demonstrates the cost breakdown of the optimal hybrid cases. The CC-controlled DG/PV/WT/HKT energy system in Lavan Island is the winning design based on the objective of the lowest NPC and COE. This system's NPC, COE, and fuel costs are $1.02 M and $0.089/kWh, respectively. The greatest NPC and COE were observed with the LF-controlled case
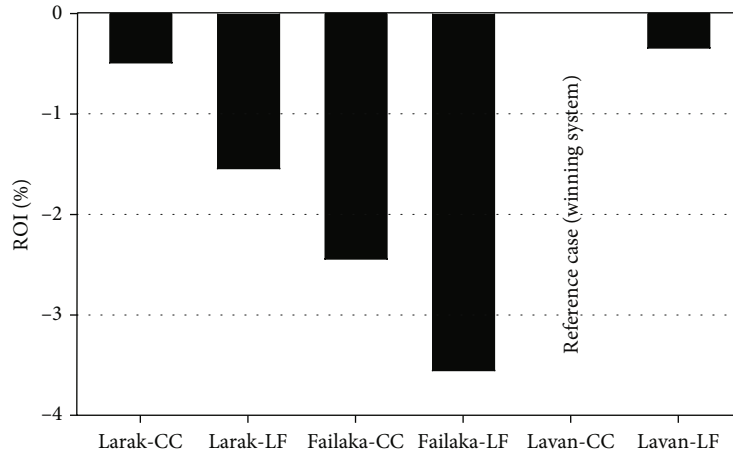
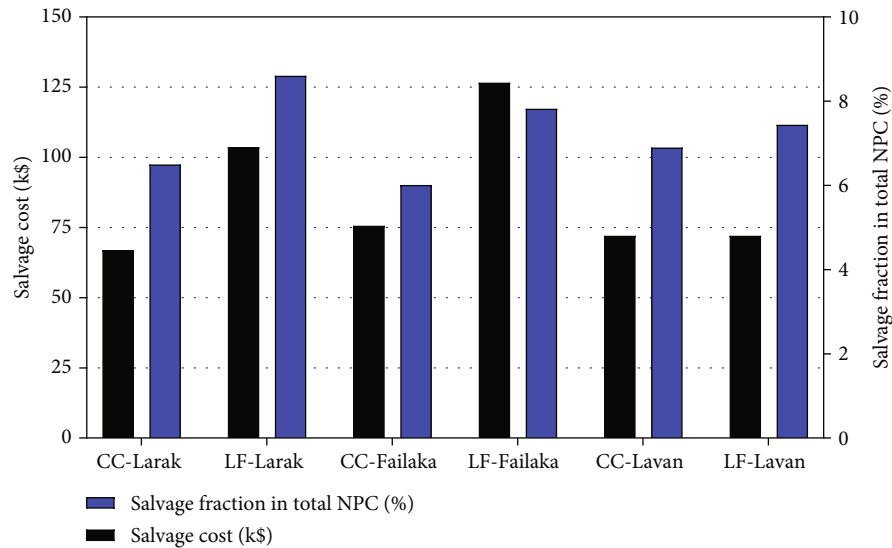FIGURE 8: Return on investment (ROI) with CC-based system in Lavan Island as the reference case.

FIGURE 9: Effects of dispatch strategy and location on the value of energy input/output of the battery.
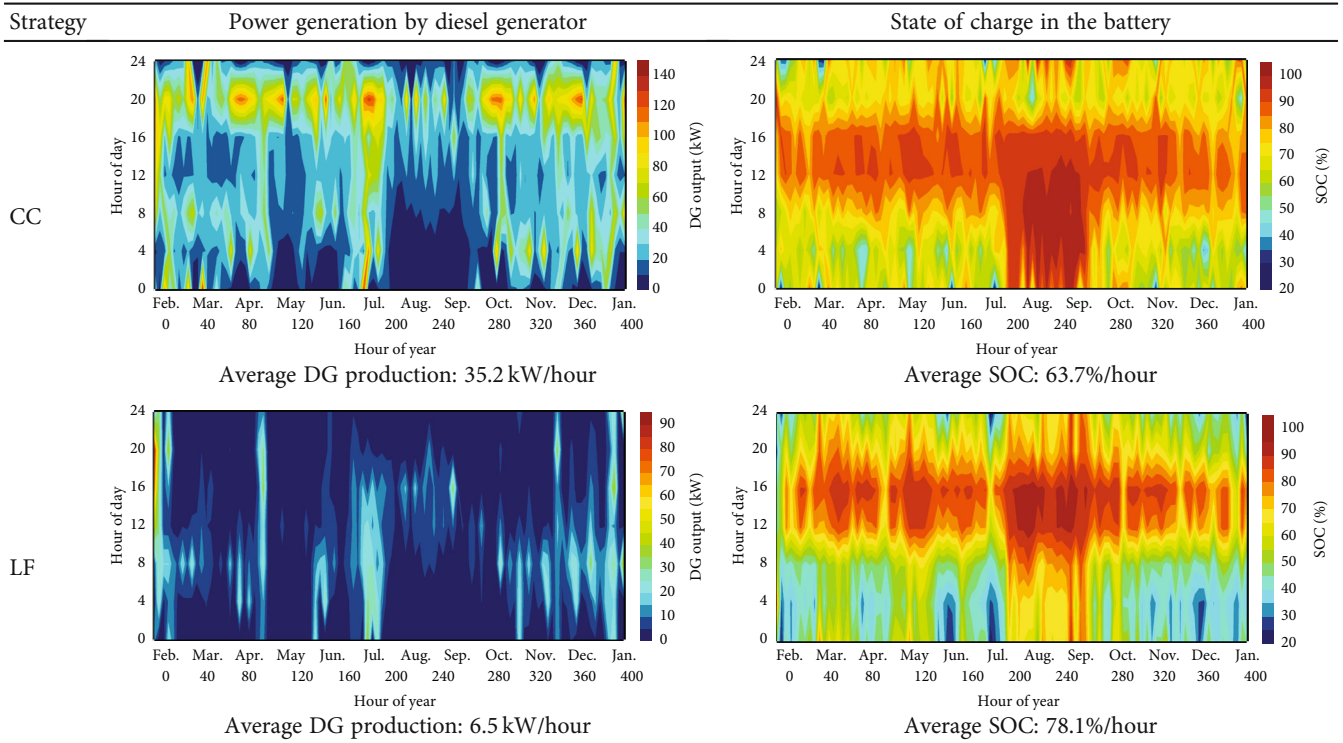
in Failaka Island, at \$1.67 M and \$0.146/kWh, respectively. The lowest NPC and COE in Failaka Island occurring under CC are, respectively, \$0.5 M and \$0.06/kWh higher than Larak Island, as well as \$0.3 M and \$0.05/kWh higher than Lavan Island. Fuel expenditure on the CC-controlled system is about four times higher than that of the LF-controlled. In fact, the CC dispatch strategy tends to use the diesel generator's highest capacity to satisfy the required load. It then results in lower utilization of renewables and higher operation hour of the generator, compared to the LF strategy. Note that among considered areas, the fuel cost in Failaka Island is more than other islands, which can be due to greater fuel prices in Kuwait (\$0.381/L) than that in Iran (\$0.122/L). The LF-controlled system in Failaka Island has the highest and lowest O&M cost and capital cost, respectively. Equipment replacement in Larak Island on average is more expensive compared to other systems.

The annual savings related to capital expenditure are referred to as the return on investment (ROI). The negative ROI of the project implies that we cannot earn sufficient

money back to recover the initial expenditures. When the ROI value is positive, the investor can make a profit on the funds invested. Figure 8 depicts the ROI under each dispatch strategy in the selected areas compared to the winning case, which is the CC-based system in Lavan Island. All optimal solutions under CC and LF demonstrate negative ROI values. This can be primarily as a result of the high initial expenditure at the year zero of the project. Failaka cases (LF- and CC-based) show the lowest profitability than the reference case.

3.1.2. Generator and Battery Status. The total energy that cycles through the batteries for a year is expressed as battery throughput (kWh). The average energy (kWh) between energy in and out is used to estimate battery throughput. Battery throughput can provide information about the battery's operational lifetime; annual throughput and battery lifetime have an inverse correlation. Figure 9 depicts the battery input/output energies under CC and LF controllers. Here, the total energy charged to the store (energy in) is more than the amount of energy released from the storage

TABLE 7: The annual performance of generator and battery under CC and LF dispatch strategies.

Strategy	Power generation by diesel generator	State of charge in the battery
CC	Average DG production: 35.2 kW/hour	Average SOC: 63.7%/hour
LF	Average DG production: 6.5 kW/hour	Average SOC: 78.1%/hour

(energy out). CC strategy takes priority to keeping higher SOC and gets charged at the full DG capacity, resulting in higher energy levels than the LF controller. The CC-based battery in Lavan Island and LF-based battery in Larak Island are expected to operate better over a longer and shorter lifetime, respectively. It should be concluded that the LF-controlled battery would need more replacement times than the of CC-controlled.

Table 7 shows the yearly performance of DG and battery performance under various dispatch strategies. Because of the pattern of the LF method, the principal aim of the DG is to satisfy a portion of the required load; the capacity of the HES is influenced by the need of the battery units, deferrable load, and remaining portions of the primary load. While the CC controller operates a generator to satisfy its maximum power regardless of how much load requirement is. Therefore, a CC-controlled generator is utilized higher than that of LF-controlled during a year. Because diesel provides power during peak hours, produced electricity is more economical; therefore, more generator operating hours are used in the optimal system. The electricity of LF-controlled batteries is met by renewables, while CC-controlled batteries depend on the DG's excess electricity. In this case, the average SOC of the LF-controlled battery is 14.5% higher compared to the CC-controlled battery.

3.1.3. Emission Gases Measurement. It is critical to measure the harmful gaseous pollutants emitted by diesel use that negatively impact the environment and human health. These dangerous gas emissions consist of NO_x, SO_2, PM, UHC, CO, and CO_2. Figure 10 compares the yearly emissions of
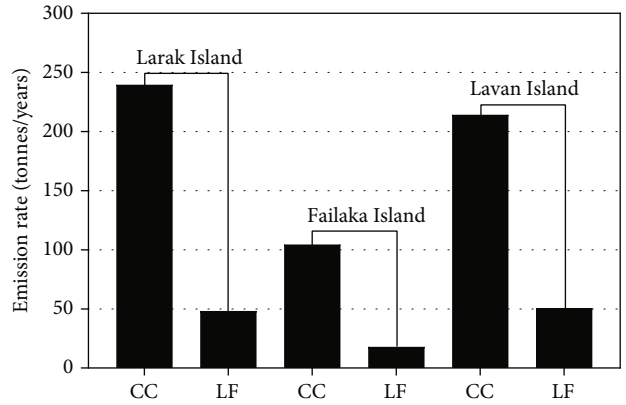

FIGURE 10: Emissions rates of the optimum solutions in LF and CC strategies.

the CC- and LF-controlled winning options on each island. As expected, the results indicate that CC-controlled options have greater gas emissions than that LF-controlled due to the higher generator use. The CC- and LF-controlled systems in Failaka Island see environmentally friendlier electricity generation by 57% and 54% less emissions than Larak and Lavan, respectively.

3.2. Sensitivity Evaluation. The sensitivity analysis of the optimum cases is discussed in this part, which determines whether dispatch techniques (LF and CC) are affected during input data fluctuation. It allows users to predict and generalize how the energy option is more likely to change in different environmental, financial, and technical conditions.
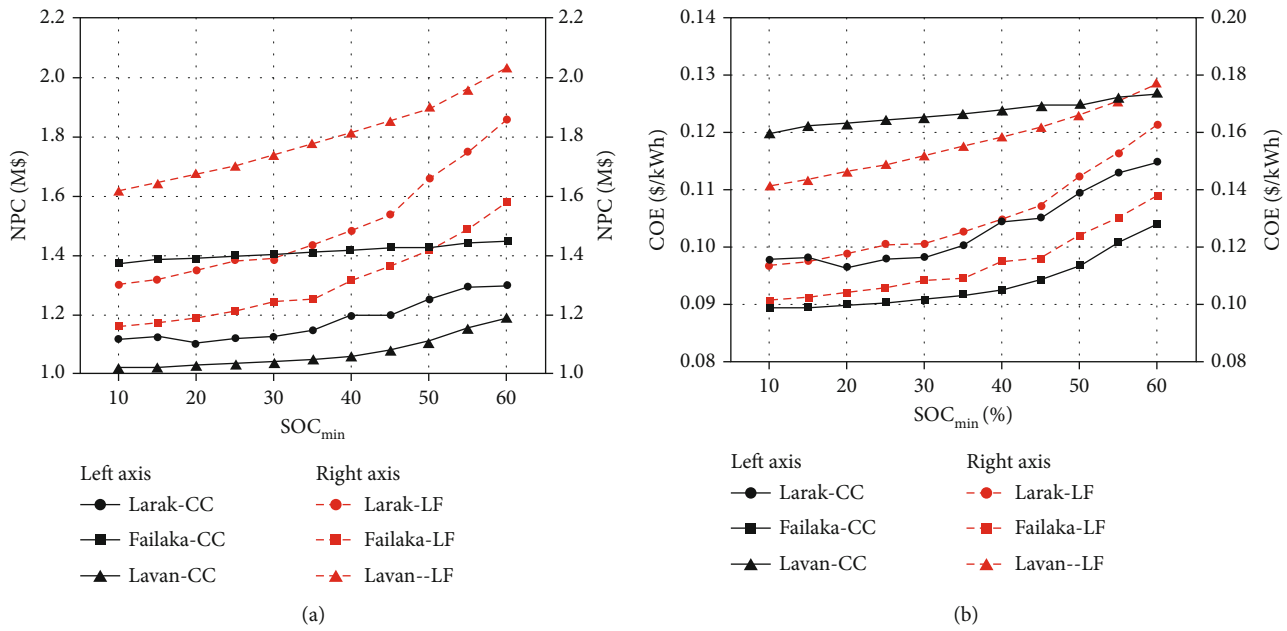
FIGURE 11: Effects of SOC_{min} on (a) present cost and (b) energy cost of the optimal solutions.
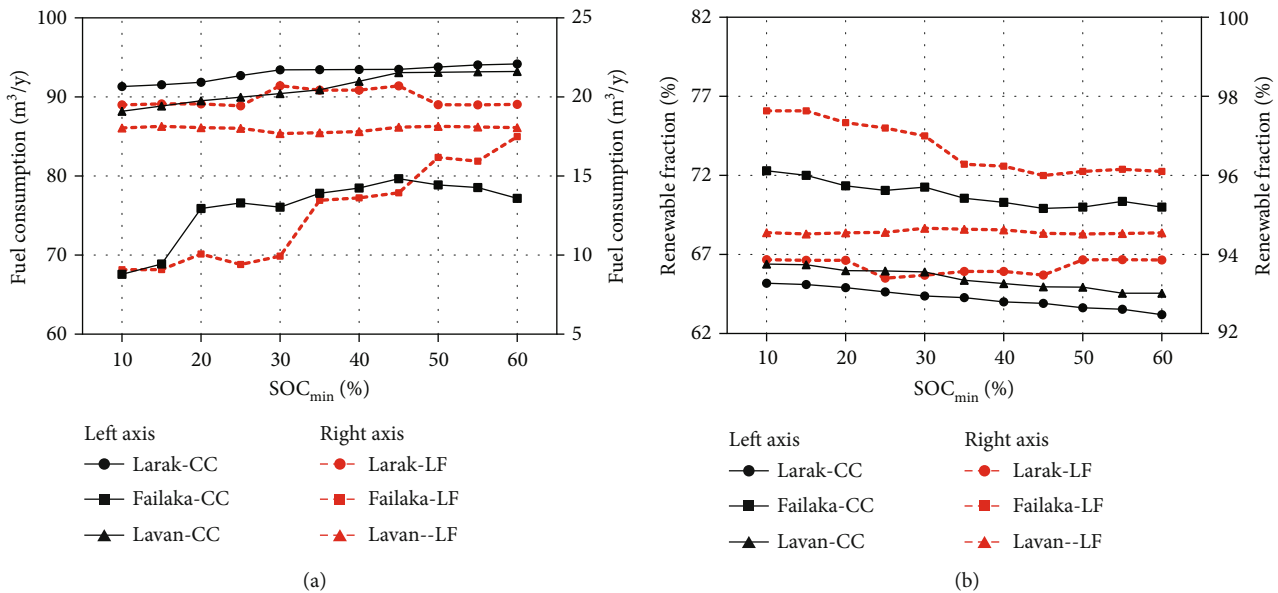

FIGURE 12: Impacts of SOC_{min} on (a) fuel use and (b) renewable fraction of the optimal solutions.

3.2.1. Effects of SOC_{min} on Technical and Financial Parameters. The effects of the minimum state of battery charge (SOC_{min}) on associated expenses and fuel usage are discussed. SOC_{min} is expressed as a level of charge under which the storage capacity cannot be discharged—changing SOC_{min} influences NPC and COE of optimal systems, as shown in Figures 11(a) and 11(b). Since LF controller needs greater energy from renewables, they demand more power from the battery, resulting in larger battery units and greater present cost compared with CC controllers. Once the LF-controlled battery has higher SOC_{min} (less capacity), the system would have to utilize more DG operation, raising

the system investment. Here, the COE increases from $0.001/kWh to $0.004/kWh in CC and from $0.004/kWh to $0.01/kWh in LF strategy for every 5% rise in SOC_{min}.

The electricity generated by renewables is proportional to renewable resources; thus, fluctuation in renewable conditions affects finances and technical performance. Figures 12(a) and 12(b) demonstrate the impacts of the SOC_{min} on fuel use and the renewable penetration of each optimal solution. An increase in SOC_{min} in LF and CC strategies grows dependence on the generator in meeting the load resulting in a rise in fuel consumption. More DG operation hour lowers the renewable fraction of HES under both
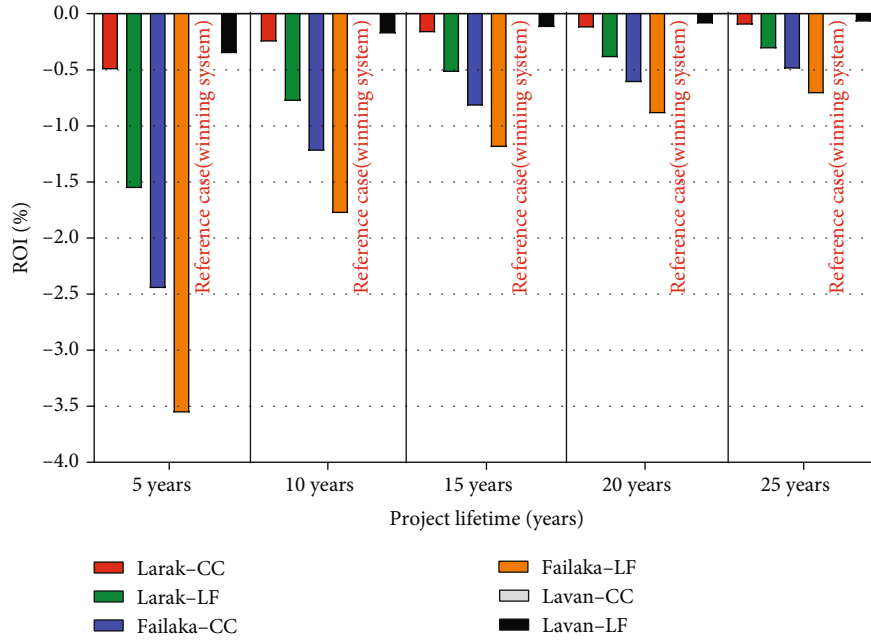
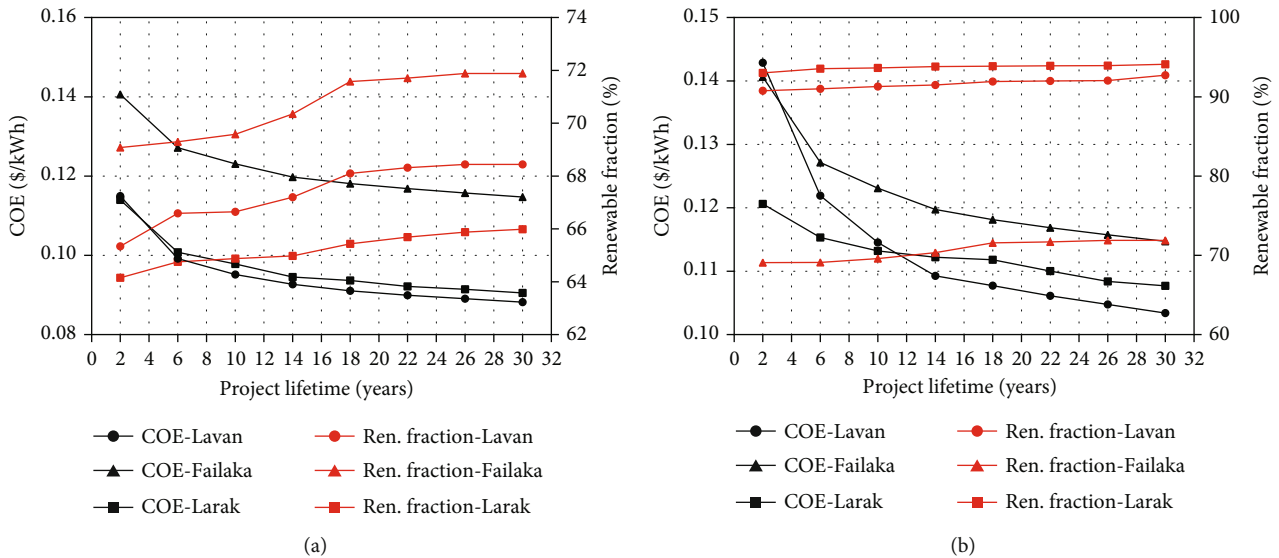FIGURE 13: The impacts of project lifetime on the ROI values of the target areas.

(a)

(b)

FIGURE 14: The impact of lifetime on the COE and the renewable fraction of in (a) CC-controlled and (b) LF-controlled system.

controlling strategies. The highest and lowest rise in fuel use is in the CC-controlled case in Failaka Island ($\sim 2.5\,m^3/yr$) and the LF-controlled case in Lavan Island ($\sim 0.005\,m^3/yr$), respectively. Because the CC strategy firstly satisfies the required load with the full generator capacity and excess energy is drawn into the battery, variation of SOC_{min} highly impacts CC-based systems.

3.2.2. Effects of Project Lifetime on Technical and Financial Indicators. Figure 13 displays the impacts of the project lifetime on the values of ROI in target islands. The longer the project lifetime, the higher cost-effectiveness the project witnesses. All cases in 25 years of the project lifetime obtain the ROI lowest than -1% ROI. LF-controlled systems have

more negative ROI values than that of CC-controlled. This trend shows that the longer lifetime of the hybrid renewable options would give higher cost-effectiveness for returning the project's initial expenses.

Figures 14(a) and 14(b) demonstrate the impact of project lifetime on the renewable fraction energy cost of the optimum solutions under CC and LF controlling methods. As the project duration grows in all islands, the COE decreases, and the renewable fraction of the final electricity generated rises. Over the lifetime increment, the rise in the renewable fraction values of LF-controlled systems is slightly lower than that of CC-controlled. The highest reduction of COE occurs for the LF-based system of Lavan Island by 23% and 28% under CC and LF dispatch strategies.
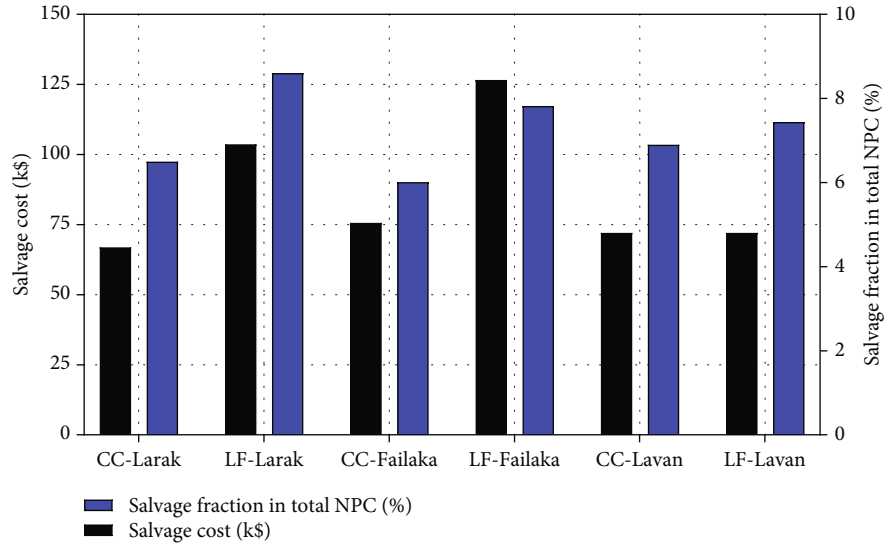
FIGURE 15: A comparison of the salvage value in the total present and its value in CC and LF methods.
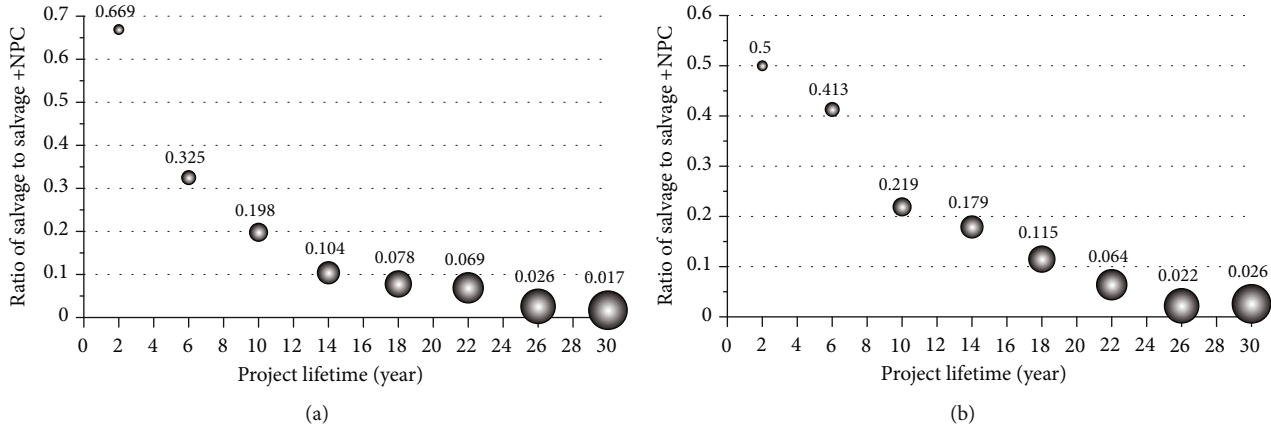

FIGURE 16: Effects of project lifetime on the share of salvage value in NPC for (a) CC- and (b) LF-controlled HES.

3.3. Salvage Value Evaluation. Figure 15 demonstrates the comparison of the salvage fraction in the total net present and its cost value under various dispatch strategies. None of the values for salvage fraction over NPC can exceed 10%. Further, the portion of the salvage fraction in the CC method is lower, shifting from 6% to 7% of the NPC. The use of the LF strategy, due to a higher number of solar panels in its optimal solution, results in a higher proportion of the salvage (between 6% and 8%). The highest and lowest salvage cost is pertinent to the CC-based option in Larak (~$67 k) and the LF-based option in Failaka Island (~$127 k), respectively.

Figures 16(a) and 16(b) illustrate the impacts of the project lifetime on the salvage share in the NPC in the CC and LF method, respectively. The disparity in the size of the bubbles shows that once the project lifetime increases under both controlling methods, the NPC rises. The ratio of the salvage to the sum of the present cost and salvage, on the other hand, would drop as the project lifetime increases. This diagram reveals that the portion of salvage in the short-term is higher than that of the long-term pro-

ject, demonstrating higher profitability of the long-term consideration of project. The cause for this trend is that the remaining lifetime of the components in a short-term project is significant; hence, the volatility of the selling prices would significantly impact the outcomes.

4. Conclusion

The principal goal of this article is to determine technically viable and economically viable hybrid energy options for a standalone electrification plan of 200 rural households in three remote islands of Persian Gulf. The main part of the investigation focused on comparing the impacts of CC and LF strategies, project lifetime, renewable resources, and SOC_{min}. The integration of the CC-controlled energy solution in Lavan Island revealed the lowest NPC and was called a winning solution. However, it did not demonstrate the positive environmental-friendly outcomes that other areas in terms of emitting CO_2 emissions. This winning configuration embodies a 150 kW DG, 349 kW PV panels, 2 hydroturbines, 1 wind turbine, 316 kWh battery, and 323 kW system

converter. The winning case minimizes net present cost by 9% and 39% than CC-controlled options of Larak and Failaka Island, respectively. Every 5% growth of SOC_{min} raises COE from \$0.001/kWh to \$0.004/kWh in CC and from \$0.004/kWh to \$0.01/kWh in the LF method. The highest and lowest growth in fuel use because of SOC_{min} is seen in the CC-controlled solution in Failaka Island (~2.5 m^3/yr) and the LF-based system in Lavan Island (~0.005 m^3/yr), respectively. The ROI comparison of the winning case with other systems indicated that all optimal solutions obtain negative ROI values. Failaka cases (LF and CC-based) reveal the lowest cost-effectiveness than the reference case. As the project duration goes up, the COE decreases, however, the fraction of the renewable energy output rises. The rise in the renewable fraction values of LF-controlled systems is slightly lower than that of CC-controlled. The highest reduction of COE occurs for the LF-based system of Lavan Island by 23% and 28% under CC and LF dispatch strategies. Hybrid energy systems are recommended to be implemented under a longer project lifetime (>20 years) to achieve more profitable results. Researchers with relevant studies are encouraged to evaluate the influence of salvage value on hybrid energy system optimization in order for more precise findings to obtain.

For future research, the impact of adopting other controlling techniques on HES with multiple fuel generators can be explored.

Data Availability

No supporting data is available.

Additional Points

Highlights. (i) Optimal sizing of off-grid PV/WT/HKT/DG system is conducted for remote islands. (ii) Performance analysis of CC and LF-controlled renewable systems is performed. (iii) CC-based systems are superior to of LF-based in minimizing present cost. (iv) LF-based designs produce lower emissions than of CC mode. (v) Higher project lifetime demonstrates higher profitability in two controlling strategies.

Conflicts of Interest

The authors declare that they have no conflicts of interest.

References

[1] L. Zhang, H. Xin, H. Yong, and Z. Kan, "Renewable energy project performance evaluation using a hybrid multi-criteria decision-making approach: case study in Fujian, China," *Journal of Cleaner Production*, vol. 206, pp. 1123–1137, 2019.

[2] F. Martin-Martínez, A. Sánchez-Miralles, and M. Rivier, "A literature review of microgrids: a functional layer based classification," *Renewable and Sustainable Energy Reviews*, vol. 62, pp. 1133–1153, 2016.

[3] S. A. Sadat, J. Faraji, M. Babaei, and A. Ketabi, "Techno-economic comparative study of hybrid microgrids in eight climate zones of Iran," *Energy Science & Engineering*, vol. 8, no. 9, pp. 3004–3026, 2020.

[4] W. S. Hassanein, M. M. Ahmed, M. O. abed el-Raouf, M. G. Ashmawy, and M. I. Mosaad, "Performance improvement of off-grid hybrid renewable energy system using dynamic voltage restorer," *Alexandria Engineering Journal*, vol. 59, no. 3, pp. 1567–1581, 2020.

[5] J. Widén, E. Wäckelgård, and P. D. Lund, "Options for improving the load matching capability of distributed photovoltaics: methodology and application to high-latitude data," *Solar Energy*, vol. 83, no. 11, pp. 1953–1966, 2009.

[6] M. Arabzadeh Saheli, K. Lari, and S. B. Kasaeian Ziarati, "Techno-economic feasibility of a standalone hybrid energy system for semi equatorial climates: a case study," *International Journal of Green Energy*, vol. 16, no. 14, pp. 1131–1143, 2019.

[7] R. Logesh, "Resources, configurations, and soft computing techniques for power management and control of PV/wind hybrid system," *Renewable and Sustainable Energy Reviews*, vol. 69, pp. 129–143, 2017.

[8] M. B. Jamnani, D. S. K. Ting, R. Carriveau, and A. Kardgar, "Energy, exergy, environmental (3E) and parametric assessment of a triple-pressure reheat combined-cycle power plant," *Journal of Energy Resources Technology*, vol. 143, no. 11, article 112104, 2021.

[9] M. Babaei Jamnani and A. Kardgar, "Energy-exergy performance assessment with optimization guidance for the components of the 396-MW combined-cycle power plant," *Energy Science & Engineering*, vol. 8, no. 10, pp. 3561–3574, 2020.

[10] O. Nematollahi, H. Hoghooghi, M. Rasti, and A. Sedaghat, "Energy demands and renewable energy resources in the Middle East," *Renewable and Sustainable Energy Reviews*, vol. 54, pp. 1172–1181, 2016.

[11] H. A. Fakhim and M. F. Sarir, "Economic feasibility of power supply using hybrid system for a hotel in cold climate," *International Journal of Energy Economics and Policy*, vol. 7, no. 2, pp. 255–261, 2017.

[12] A. Kordvani, M. Hassan, L. Dalton, and P. Berenjforoush, *Renewable Energy in Iran*, SATBA, 2017, http://www.satba.gov.ir/suna_content/media/image/2017/02/5196_orig.pdf?t=636219021775330000.

[13] H. J. Vermaak, "Techno-economic analysis of solar tracking systems in South Africa," *Energy Procedia*, vol. 61, pp. 2435–2438, 2014.

[14] K. Kusakana, "Optimal operation scheduling of a hydrokinetic-diesel hybrid system with pumped hydro storage," in *2015 4th International Conference on Electric Power and Energy Conversion Systems (EPECS)*, Sharjah, United Arab Emirates, 2015.

[15] K. Kusakana, "Optimization of the daily operation of a hydrokinetic-diesel hybrid system with pumped hydro storage," *Energy Conversion and Management*, vol. 106, pp. 901–910, 2015.

[16] H. J. Vermaak, K. Kusakana, and S. P. Koko, "Status of micro-hydrokinetic river technology in rural applications: a review of literature," *Renewable and Sustainable Energy Reviews*, vol. 29, pp. 625–633, 2014.

[17] M. H. Jahangir, A. Shahsavari, and M. A. Vaziri Rad, "Feasibility study of a zero emission PV/wind turbine/wave energy converter hybrid system for stand-alone power supply: a case study," *Journal of Cleaner Production*, vol. 262, article 121250, 2020.

[18] A. Razmjoo and A. Davarpanah, "Developing various hybrid energy systems for residential application as an appropriate and reliable way to achieve energy sustainability," *Energy Sources, Part A: Recovery, Utilization, and Environmental Effects*, vol. 41, no. 10, pp. 1180–1193, 2019.

[19] M. R. Akhtari and M. Baneshi, "Techno-economic assessment and optimization of a hybrid renewable co-supply of electricity, heat and hydrogen system to enhance performance by recovering excess electricity for a large energy consumer," *Energy Conversion and Management*, vol. 188, pp. 131–141, 2019.

[20] M. H. Jahangir, S. A. Mousavi, and M. A. Vaziri Rad, "A techno-economic comparison of a photovoltaic/thermal organic Rankine cycle with several renewable hybrid systems for a residential area in Rayen, Iran," *Energy Conversion and Management*, vol. 195, pp. 244–261, 2019.

[21] W. Zhang, A. Maleki, M. A. Rosen, and J. Liu, "Optimization with a simulated annealing algorithm of a hybrid system for renewable energy including battery and hydrogen storage," *Energy*, vol. 163, pp. 191–207, 2018.

[22] D. Guangqian, K. Bekhrad, P. Azarikhah, and A. Maleki, "A hybrid algorithm based optimization on modeling of grid independent biodiesel-based hybrid solar/wind systems," *Renewable Energy*, vol. 122, pp. 551–560, 2018.

[23] Q. Ma, X. Huang, F. Wang, C. Xu, R. Babaei, and H. Ahmadian, "Optimal sizing and feasibility analysis of grid-isolated renewable hybrid microgrids: effects of energy management controllers," *Energy*, vol. 240, article 122503, 2022.

[24] M. Ramesh and R. P. Saini, "Dispatch strategies based performance analysis of a hybrid renewable energy system for a remote rural area in India," *Journal of Cleaner Production*, vol. 259, article 120697, 2020.

[25] K. Murugaperumal, S. Srinivasn, and G. R. K. D. Satya Prasad, "Optimum design of hybrid renewable energy system through load forecasting and different operating strategies for rural electrification," *Sustainable Energy Technologies and Assessments*, vol. 37, article 100613, 2020.

[26] A. Cano, P. Arévalo, and F. Jurado, "Energy analysis and techno-economic assessment of a hybrid PV/HKT/BAT system using biomass gasifier: Cuenca-Ecuador case study," *Energy*, vol. 202, p. 117727, 2020.

[27] M. D. Hossen, M. F. Islam, M. F. Ishraque, S. A. Shezan, and S. M. Arifuzzaman, "Design and implementation of a hybrid solar-wind-biomass renewable energy system considering meteorological conditions with the power system performances," *International Journal of Photoenergy*, vol. 2022, Article ID 8792732, 17 pages, 2022.

[28] N. Ganjei, F. Zishan, R. Alayi et al., "Designing and sensitivity analysis of an off-grid hybrid wind-solar power plant with diesel generator and battery backup for the rural area in Iran," *Journal of Engineering*, vol. 2022, Article ID 4966761, 14 pages, 2022.

[29] N. Jha, D. Prashar, M. Rashid et al., "Energy-efficient hybrid power system model based on solar and wind energy for integrated grids," *Mathematical Problems in Engineering*, vol. 2022, Article ID 4877422, 12 pages, 2022.

[30] S. Siddula, G. K. Prashanth, P. Nandankar et al., "Optimal placement of hybrid wind-solar system using deep learning model," *International Journal of Photoenergy*, vol. 2022, Article ID 2881603, 7 pages, 2022.

[31] L. Xu, Z. Wang, Y. Liu, and L. Xing, "Energy allocation strategy based on fuzzy control considering optimal decision boundaries of standalone hybrid energy systems," *Journal of Cleaner Production*, vol. 279, article 123810, 2021.

[32] M. R. A. Refaai, S. N. R. Vonteddu, P. K. Nunna, P. S. Kumar, C. Anbu, and M. Markos, "Energy management prediction in hybrid PV-battery systems using deep learning architecture," *International Journal of Photoenergy*, vol. 2022, Article ID 6844853, 7 pages, 2022.

[33] C. Hou, H. Wang, and M. Ouyang, "Battery sizing for plug-in hybrid electric vehicles in Beijing: a TCO model based analysis," *Energies*, vol. 7, no. 8, pp. 5374–5399, 2014.

[34] A. B. Esan, A. F. Agbetuyi, O. Oghorada, K. Ogbeide, A. A. Awelewa, and A. E. Afolabi, "Reliability assessments of an islanded hybrid PV-diesel-battery system for a typical rural community in Nigeria," *Heliyon*, vol. 5, no. 5, article e01632, 2019.

[35] H. Liu, B. Wu, A. Maleki, F. Pourfayaz, and R. Ghasempour, "Effects of reliability index on optimal configuration of hybrid solar/battery energy system by optimization approach: a case study," *International Journal of Photoenergy*, vol. 2021, Article ID 9779996, 11 pages, 2021.

[36] A. Oulis Rousis, D. Tzelepis, I. Konstantelos, C. Booth, and G. Strbac, "Design of a Hybrid AC/DC microgrid using HOMER pro: case study on an islanded residential application," *Inventions*, vol. 3, no. 3, p. 55, 2018.

[37] M. Kharrich, S. Kamel, A. S. Alghamdi et al., "Optimal design of an isolated hybrid microgrid for enhanced deployment of renewable energy sources in Saudi Arabia," *Sustainability*, vol. 13, no. 9, pp. 4708–4726, 2021.

[38] M. Kharrich, S. Kamel, R. Ellaia et al., "Economic and ecological design of hybrid renewable energy systems based on a developed IWO/BSA algorithm," *Electronics*, vol. 10, no. 6, p. 687, 2021.

[39] B. Kamranzad and V. Chegini, "Study of wave energy resources in Persian Gulf: seasonal and monthly distributions," in *11th International Conference on Coasts, Ports and Marine Structures, (ICOPMAS 2014)*, pp. 658–661, Tehran, Iran, January 2015.

[40] D. Methodology, *NASA, Surface meteorology and Solar Energy*https://power.larc.nasa.gov/.

[41] B. K. Das, Y. M. Al-Abdeli, and M. Woolridge, "Effects of battery technology and load scalability on stand-alone PV/ICE hybrid micro-grid system performance," *Energy*, vol. 168, pp. 57–69, 2019.

[42] A. S. Aziz, M. F. N. Tajuddin, M. R. Adzman, M. A. M. Ramli, and S. Mekhilef, "Energy management and optimization of a PV/diesel/battery hybrid energy system using a combined dispatch strategy," *Sustainability*, vol. 11, no. 3, p. 683, 2019.

[43] L. Olatomiwa, S. Mekhilef, A. S. N. Huda, and O. S. Ohunakin, "Economic evaluation of hybrid energy systems for rural electrification in six geo-political zones of Nigeria," *Renewable Energy*, vol. 83, pp. 435–446, 2015.

[44] Products, "PEIMAR."https://www.peimar.com/us/home-us/.

[45] S. Baek, E. Park, M. G. Kim et al., "Optimal renewable power generation systems for Busan metropolitan city in South Korea," *Renewable Energy*, vol. 88, pp. 517–525, 2016.

[46] E. Muh and F. Tabet, "Comparative analysis of hybrid renewable energy systems for off-grid applications in Southern Cameroons," *Renewable Energy*, vol. 135, pp. 41–54, 2019.

[47] C. S. Lai, Y. Jia, Z. Xu et al., "Levelized cost of electricity for photovoltaic/biogas power plant hybrid system with electrical

energy storage degradation costs," *Energy Conversion and Management*, vol. 153, pp. 34–47, 2017.

[48] T. Salameh, M. A. Abdelkareem, A. G. Olabi, E. T. Sayed, M. Al-Chaderchi, and H. Rezk, "Integrated standalone hybrid solar PV, fuel cell and diesel generator power system for battery or supercapacitor storage systems in Khorfakkan, United Arab Emirates," *International Journal of Hydrogen Energy*, vol. 46, no. 8, pp. 6014–6027, 2021.

[49] D. N. Luta and A. K. Raji, "Decision-making between a grid extension and a rural renewable off-grid system with hydrogen generation," *International Journal of Hydrogen Energy*, vol. 43, no. 20, pp. 9535–9548, 2018.

[50] B. K. Das, N. Hoque, S. Mandal, T. K. Pal, and M. A. Raihan, "A techno-economic feasibility of a stand-alone hybrid power generation for remote area application in Bangladesh," *Energy*, vol. 134, pp. 775–788, 2017.

[51] Y. Hong, R. Waters, C. Boström, M. Eriksson, J. Engström, and M. Leijon, "Review on electrical control strategies for wave energy converting systems," *Renewable and Sustainable Energy Reviews*, vol. 31, pp. 329–342, 2014.

[52] T. Aderinto and H. Li, "Ocean wave energy converters: status and challenges," *Energies*, vol. 11, no. 5, p. 1250, 2018.

[53] M. Baneshi and F. Hadianfard, "Techno-economic feasibility of hybrid diesel/PV/wind/battery electricity generation systems for non-residential large electricity consumers under southern Iran climate conditions," *Energy Conversion and Management*, vol. 127, pp. 233–244, 2016.

[54] D. N. Luta and A. K. Raji, "Optimal sizing of hybrid fuel cell-supercapacitor storage system for off-grid renewable applications," *Energy*, vol. 166, pp. 530–540, 2019.

[55] A. Toopshekan, H. Yousefi, and F. R. Astaraei, "Technical, economic, and performance analysis of a hybrid energy system using a novel dispatch strategy," *Energy*, vol. 213, p. 118850, 2020.

[56] L. M. Halabi and S. Mekhilef, "Flexible hybrid renewable energy system design for a typical remote village located in tropical climate," *Journal of Cleaner Production*, vol. 177, pp. 908–924, 2018.